ESKİŞEHİR TEKNİK ÜNİVERSİTESİ BİLİM VE TEKNOLOJİ DERGİSİ B- TEORİK BİLİMLER

Eskişehir Technical University Journal of Science and Technology B- Theoretical Sciences

2023, 11(1), pp. 43-55, DOI: 10.20290/estubtdb.1126604

RESEARCH ARTICLE

DFT CALCULATIONS AND MOLECULAR DOCKING STUDY IN 6-(2"-PYRROLIDINONE-5"-YL)-(-) EPICATECHIN MOLECULE FROM FLAVONOIDS

Mehmet BAĞLAN [1,*], Ümit YILDIKO [2], Kenan GÖREN [1]

[1]Department of Chemistry, Kafkas University, Kars 36100, Turkey
[2]Department of Bioengineering, Kafkas University, Kars 36100, Turkey

ABSTRACT

The 6-311G(d,p) and SDD basis sets have been used to calculate the vibration frequencies, and the DFT/B3LYP approach was used to optimize the structure. The energy gap of the molecule has been calculated using the lowest unoccupied molecular orbital (LUMO) with the highest occupied molecular orbital (HOMO). The stability and charge delocalization of the Title molecule have been investigated using natural bond orbital (NBO) analysis. The dipole moment, polarizability, and first-order hyperpolarizability, as well as the molecular electrostatic potentially (MEP) and thermodynamic features, have been used to compute the nonlinear optical (NLO) behavior of the title molecule. The Schrödinger program was used to conduct molecular docking works to determine information about the interactions between the AChE and BChE enzymes and the chemical. In addition, a molecular docking study was analyzed for compounds 6-(2"-Pyrrolidinone-5"-yl)-(-)epicatechin (PEP) with AChE and BChE synthase binding proteins (PDB:4M0E) and (PDB:6SAM) using the Discovery Studio 2021 Client program. In the compound, the AChE enzyme showed -7.105 kcal/mol, while the BChE enzyme showed a result score of -7.784 kcal/mol.

Keywords: PEP, DFT, HOMO-LUMO, NBO, Molecular docking

1. INTRODUCTION

Flavonoid alkaloids, unlike others, are a natural product. Almost always, flavonoids contain five or six-membered nitrogen heterocycles attached to the C6 and C8 places of the ring in their skeleton [1]. Most of the compounds in this category can be optained in plants used in traditional medicine as herbal medicine for various ailments [2]. Some substances have been found to have beneficial pharmacological properties [3]. Research on flavonoid alkaloids has drawn even more attention to the fact that it is a synthetic derivative of flavonoid alkaloids, flavopiridol. The synthesis and The isolation of flavonoid alkaloids and their variants is a very relevant research topic today because of the as yet untapped potential for bioactivity and structural diversity inherent in this family of natural compounds [4]. PEP is a derivative of flavan-3-ol (-)-epicatechin [5].

D.S. Jang and colleagues identified the flavonoid from the roots of Actinida arguta in 2009 [6]. The perennial vine Actinidia arguta (also known as hardy kiwi) is endemic to northern China, Japan, Korea, and Siberia [7]. It grows a fruit like kiwi that is believed to boost general health in Chinese's traditional medicine. In *in-vitro* biological investigations, the compound PEP was revealed to exhibit a considerable inhibitory effect against diabetic complications' the formation, cataracts, atherosclerosis's (AGEs) end products [8].

In physics, chemistry, and materials science, density functional theory (DFT) is a computational quantum mechanical modeling tool used to examine the electronic structure (or nuclear structure) of atoms, molecules, and dense phases in a variety of ways [9]. With advances in technique and applications, it is now possible to acquire high-quality predicted attributes such as lattice constants,

*Corresponding Author: mehmetbaglan36@gmail.com
Receievd:06.06.2022 Published: 28.02.2023

cohesion/absorption energies, band structures, surface reactivity, thermochemistry, rate constants, and other physical and chemical parameters [10, 11]. As a result, the microscopic mechanism can be analyzed by constructing interaction models between different components. A set of necessary parameters can be obtained computationally without compromising the integrity of the system, which greatly complements the experimental work and even ventures into previously unexplored areas with confidence.

In this study, B3LYP/6-311G(d,p) and B3LYP/SDD methods have been used to investigate the PEP molecule theoretically. In this study, B3LYP/6-311G(d,p) and B3LYP/SDD methods have been used to investigate the PEP molecule theoretically. The MEP surface was visualized and simulated. The title compound's molecular characteristics were computed, including polarizability, dipole moment, first-order hyperpolarizability, and thermodynamic parameters. DFT calculations with a base set were also used to compute the energy of the Highest Occupied Molecular Orbit (HOMO) and the Lowest Occupied Molecular Orbit (LUMO). The interaction between the molecules and the ligand molecule's target binding site was determined using the findings of molecular docking experiments. It was discovered what the minimal binding energy was. PEP, one of the flavonoid derivatives, was discovered in plants used as herbal therapy for numerous diseases in traditional medicine, according to the literature study. Thus, the studied compound was interlock with AChE and BChE protein.

2. MATERIALS AND METHODS

The B3LYP/6-311G(d,p) and B3LYP/SDD techniques were used to do all of the DFT calculations, which were done in Gaussian 09 software [12, 13]. For conformational analysis, a quasi-experimental technique was adopted. The shape of the final molecule was optimized as the initial stage in the computer analysis. In particular, it requires low energy sensitivity to changes in molecular structure caused by core position displacement of PEP [14]. The DFT technique in the Gaussian 09 software was used to compute the optimum geometries, vibration frequencies, and energies of the molecular structure of PEP [15]. Lee's-Yang-Parr correlation function was formed based on 6-311G(d,p) and SDD basic set based program package with DFT/B3LYP method. GaussView 6.0.16 and ChemBio Ultra Drive 3D have been used to prepare and import the visualization and input file. Molecular docking was also used to investigate the ligand's exact binding location and mechanism on the protein (using the Schrödinger, LLC model's Maestro Molecular Modeling platform (version 11.8)). Acetylcholinesterase (AChE) and Butyrylcholinesterase (BChE) enzymes obtained high resolution (2.00 Å) and (2.50 Å) crystal structures, respectively (see https://www.rcsb.org/pbd). Ligand constructs were obtained individually from the PubChem website as SDF files. It was synthesized using the previous implementation of the Ligprep module. Waited to receive data for protein preparation in the wizard module. In the meantime, all water molecules were separated as a crystal structure. The protein ion balance was adjusted by addressing this module again, this time by selecting the active site for flexible binding of the protein. Network boxes were created as the basis of the receptor networking module, allowing flexible docking by forming networks at the protein's binding sites. Network boxes have been created as the basis of the receptor networking module, allowing flexible docking by forming networks at binding sites of the protein. The highest binding affinity is indicated by the lowest energy configurations. Discovery Studio 4.5 was used to show the 2D and 3D interactions as well as the receptor model that occurred.

3. RESULTS AND DISCUSSION

3.1. Structure Details and Analysis

Figures 4a and 4b were showed the optimized chemical structure and bond length of 6-(2"-Pyrrolidinone-5"-yl)-(-)epicatech (PEP) [16, 17]. The optimal bond lengths of the molecule determined using the 6-311G (d,p) and SDD basis sets and the B3LYP/B3LYP method have been shown in Table 1. If it is a PEP compound, the bond parameters calculated by two different methods are compared with

each other. In phenyl rings, all bond lengths and angles are within typical limits. C-C bond distances range from 1.387-1.545 Å to the 6-311 G(d,p) base set and between 1.395-1.354 Å for the SDD base set. The C-N bond lengths between the phenyl rings of the nitrogen atom were found to be 1.367-1.373. The N-H distance in the structure was 1.008-1.014 Å. The C-H lengths in the aromatic ring vary from 1.086 to 1.088, whereas the O-H bond distances are between 0.962 and 0.977. The whole C-C-C angles range 109° to 121° Å. The C-N-C angle in the compound was found to be between 115° and 116° Å. The values of the 6.311 G (d,p) and SDD basis sets differ slightly. The theoretically estimated results from the B3LYP-/6-311G(d,p) and B3LYP/SDD techniques offer a sense of how the shape of the molecules alters for specific PEP compounds.

Table 1. Theoretically, derived some of the molecule's bond lengths (Å) and bond angles (º).

Bond Lengths	**B3LYP/6-311G(d,p)**	**B3LYP /SDD**	**Bond Lengths**	**B3LYP/6-311G(d,p)**	**B3LYP/ SDD**
C1-C2	1.545	1.554	**C21-H40**	1.082	1.084
C6-C8	1.407	1.418	**C1-H28**	1.098	1.101
C1-C14	1.511	1.514	**C23-H43**	1.088	1.095
C8-C22	1.515	1.542	**C2-H29**	1.1099	1.102
C9-C11	1.392	1.403	**C22-H41**	1.102	1.105
C14-C21	1.395	1.409	**C20-H39**	1.086	1.088
C18-C20	1.387	1.401	**C2-03**	1.417	1.454
C24-C25	1.532	1.533	**C16-O17**	1.360	1.390
C16-C18	1.403	1.412	**C25-O27**	1.213	1.252
C11-C12	1.388	1.395	**C25-N26**	1.367	1.373
Bond Angles	**B3LYP/6-311G**	**B3LYP /SDD**	**Bond Angles**	**B3LYP/6-311G**	**B3LYP/ SDD**
C1-C2-C4	109.378	110.236	**C23-C22-H41**	106.967	108.762
C4-C5-C6	121.508	117.25	**H44-C24-H45**	107.431	107.653
C5-C12-C11	121.508	121.246	**C1-O13-C12**	117.202	116.463
C15-C16-O17	119.992	119.799	**C22-N26-C25**	116.025	115.744
C18-O19-H38	110.149	113.307	**C25-N26-H46**	120.933	123.679
Bond Angles	**B3LYP/6-311G**	**B3LYP /SDD**	**Bond Angles**	**B3LYP/6-311G**	**B3LYP/ SDD**
C1-C14-C21-C20	177.653	-177.577	**C23-C22-N26-H46**	165.465	168.459
C4-C2-C1-C14	177.247	-177.793	**C4-N2-C1-C15**	179.891	-175.845
O3-C2-C1- O13	-179.124	-179.401	**C9-C8-C6-O7**	-179.782	174.356

3.2. HOMO and LUMO Analysis

HOMO and LUMO are defined as the chemical structure in the major orbitals [18]. The electron donating and receiving capacity is defined by the HOMO and LUMO energy properties [19]. Kinetic stability of a molecule, optical polarizability, chemical reactivity and chemical hardness or softness are all designated by the energy disparity between HOMO and LUMO [20]. Boundary electron density can be used to predict the positions of more reactive electrons in conjugated systems and to characterize various reactions [21]. The surfaces of the boundary orbital defined the crystalline bonding architecture developed. Red represents the positive phase while green represents the negative phase. Pictorial representations of PEP based upon B3LYP/6-311G (d,p) and B3LYP/SDD and its HOMO and LUMO are shown in Figures 1 and 2. While the PEP compound's the E_{HOMO}=-6.08 eV-E_{LUMO}=-0.59 eV was used to compute by the DFT/B3LYP/6-311G (d,p) method, the E_{HOMO}= -6.34 eV - E_{LUMO} = -0.76 eV of the DFT/B3LY/SDD method was calculated. When using DFT, the estimated energy gap with the B3LYP/6-311G (d,p) and B3LYP/SDD methods is 5.49 eV and 5.58 eV, in turn. The energy different between the HOMO-LUMO sizes can be used to determine the reactivity of the molecule. It stands for the molecule's high efficient electrical activity as well as a reduced energy gap. Chemical reactivity indices are listed in Table 2.

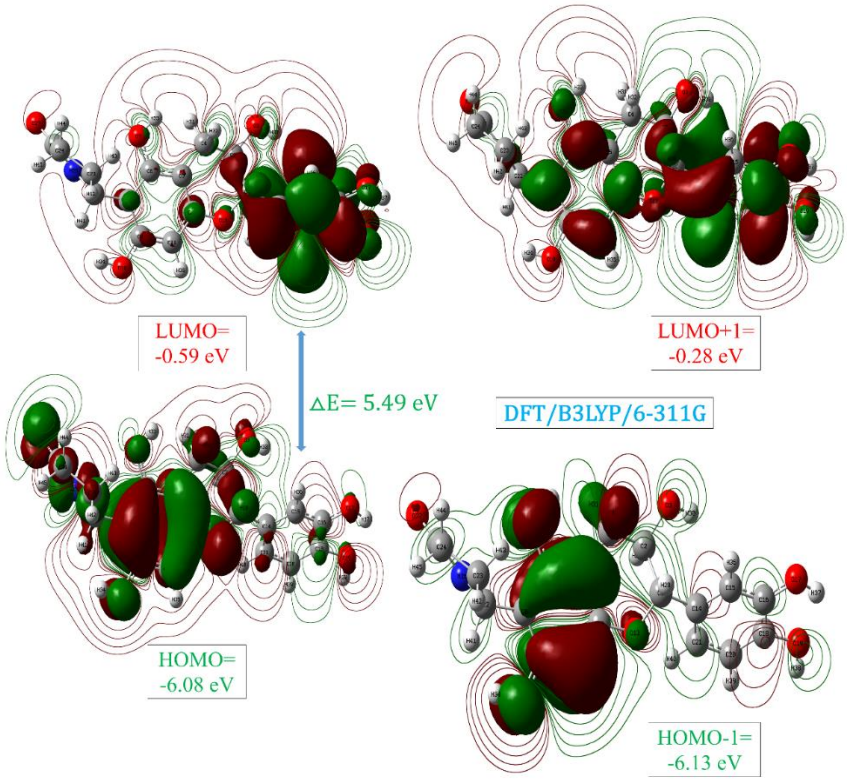

Figure 1. Boundary molecular orbitals of the PEP compound according to the DFT/B3LYP/6-311G(d,p) level.

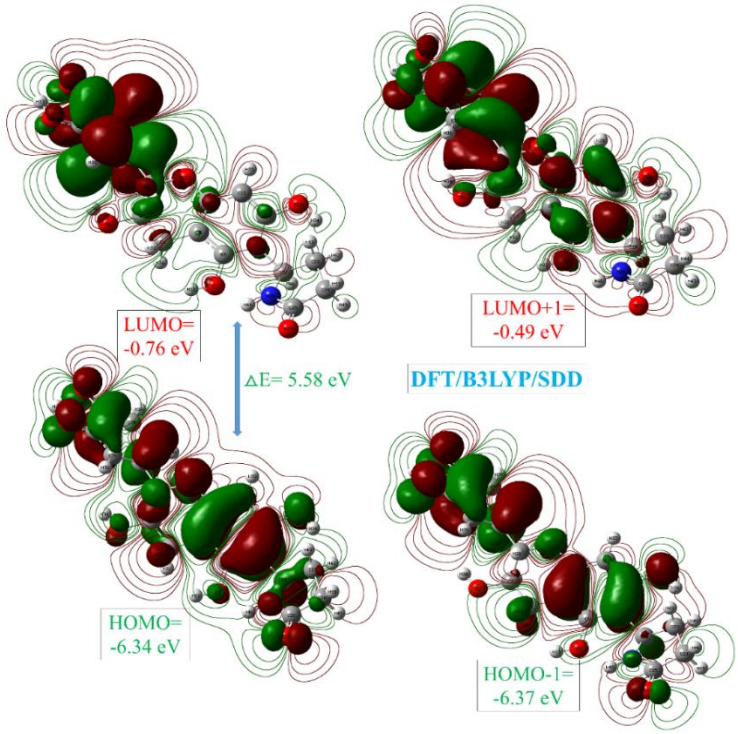

Figure 2. Boundary molecular orbitals of the PEP compound according to the DFT/B3LYP/SDD level.

Table 2. Comparison of HOMO, LUMO and chemical reactivity descriptors by DFT/B3LYP/6-311G-DFT/ B3PW91/SDD levels methods at 298.15 K in ground state.

Molecules Energy	**DFT/B3LYP/6-311G(d,p)**	**DFT/B3LYP/SDD**
E_{LUMO}	-0.5951	-0.7608
E_{HOMO}	-6.0849	-6.3423
E_{LUMO+1}	-0.2887	-0.4960
E_{HOMO-1}	-6.1312	-6.3788
Energy Gap (Δ) $\lvert E_{HOMO}- E_{LUMO}\rvert$	5.4898	5.5815
Ionization Potential ($I = -E_{HOMO}$)	6.0849	6.3423
Electron Affinity ($A = -E_{LUMO}$)	0.5951	0.7608
Chemical hardness ($\eta = (I - A)/2$)	2.7449	2.7907
Chemical softness ($s = 1/2\ \eta$)	0.1821	0.1792
Chemical Potential ($\mu = -(I + A)/2$)	-3.34	-3.5515
Electronegativity ($\chi = (1+ A)/2$)	0.7975	0.8804
Electrophilicity index ($\omega = \mu^2/2\ \eta$)	1.9987	2.2598

3.3. Molecular Electrostatic Potential (MEP)

The electric potential (considered as static charge distributions) created by the electrons in the a molecule's nucleus and the surrounding area is a very useful property for predicting and analyzing chemical reactivity behavior [22]. The potential has proven particularly effective as a predictor of which a molecule's regions or areas have been at first attracted by an approaching nucleophile and electrophile [23]. Electronic density determines the molecular electrostatic potential (MEP), which is a valuable descriptor for detecting electrophilic assault, hydrogen bond interactions and nucleophilic reactions [24]. The regions reactive to nucleophilic and electrophilic attack in the PEP compound are clearly evident in Figure 3. Different color codes can be used to locate reagent positions in MEP analysis. The red color in Figure 3 indicates an electron-rich region, which indicates the negative area in Electrophilic reactivity. The blue color in the MEP map represents an electron-deficient region indicating the positive area in Nucleophilic reactivity. In addition, the green color on the MEP map shows neutral, that is, hydrogen bond interactions and represents the zero electrostatic potential region.

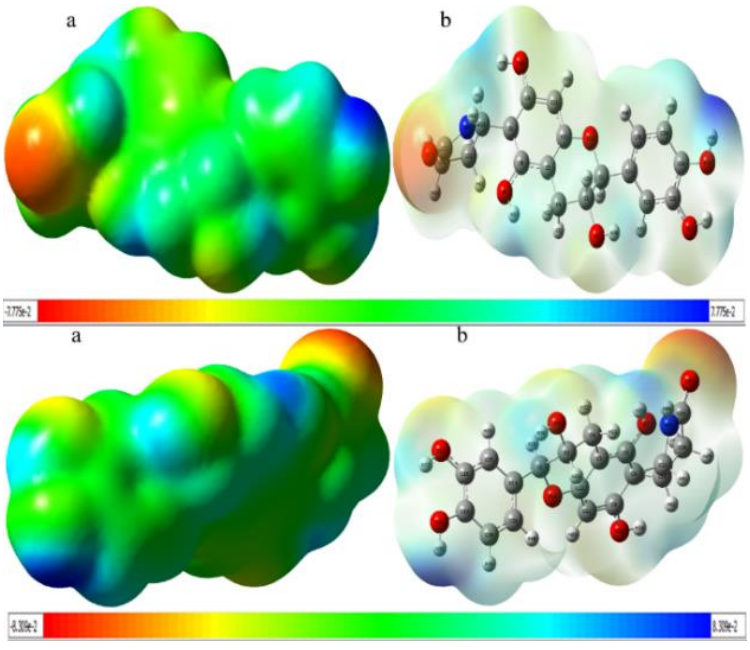

Figure 3. Molecular electrostatic potential surface by DFT/B3LYP and DFT/B3LYP methods with 6-311G(d,p) and SDD basis set

3.4. Non-Linear Optical Properties (NLO)

The molecules hyperpolarizability, chromophore density, and non-centrosymmetric order of individual organic chromophores all affect the macroscopic NLO activity of organic materials [25, 26]. Calculating the molecule's the nonlinear optical properties, using B3LYP method under SDD and 6-311G (d,p) basis sets, total static dipole moment μ, dipole moment μi component, mean polarization α, αij polarization anisotropy and first order hyperpolarizability βijk anisotropy have been calculated and the values have been presented in both atomic and electrostatic units in Table 3. B3LYP/6-311G (d,p) method with μ= 8.4176 D. α = -157.075 a.u, β=2.151x10^{-9} esu and B3LYP/SDD method with μ=8.4253 D , α=-161.068 a.u., β= 1.093x10^{-9} esu found. Its estimated values in the PEP molecule are proof that it is NLO material.

Table 3. DFT/B3LYP- B3LYP belong to 6-311G(d,p) and SDD basis set calculated dipole moments (Debye), (au) polarizability, β components, and β tot PEP value.

Parameters	B3LYP/6-311G(d,p)	B3LYP /SDD	Parameters	B3LYP/6-311G(d,p)	B3LYP /SDD
μ x	5.4098	5.6931	β XXX	480.9939	498.6413
μ y	-2.2360	-4.0763	β XXY	-205.1694	-345.1168
μ z	-0.0642	-4.4779	β XYY	16.8028	55.1368
μ (D)	5.8540	8.3114	β YYY	7.270	-3.4727
α XX	-154.1447	-157.3272	β XXZ	40.9120	-167.9551
α yy	-159.5987	-163.8682	β XYZ	-8.8088	46.5488
α zz	-155.9008	-158.6133	β YYZ	-6.4183	-25.7389
α XY	4.5393	10.7298	β XZZ	34.0086	10.3992
α XZ	-30.4499	0.8387	β YZZ	-7.8849	-3.6198
α YZ	7.4560	-2.4244	β ZZZ	-11.0534	-4.6276
α (au)	-156.5480	-159.9362	β (esu)	2.957 x10^{-8}	1.093x10^{-9}

3.5. Mulliken Atomic Charges

Mulliken obtained a natural population analysis of flavonoid derivatives. It explains how the charges are distributed in the various subshells (nucleus, valence, and Rydberg) of the molecular orbital [27, 28]. İn the table 4 has been showed the buildup of natural charges on the PEP compound's each atom. The dipole moment, electronic structure, polarizability and a system's other molecular properties are all affected by atomic charge. Atoms represented by colors according to their Mulliken charges and other images are shown in Figure 4.

Table 4. DFT/B3LYP and B3PW91 techniques with 6-311G(d,p) and SDD base set computed Mulliken atomic charges.

	B3LYP/6-311G(d,p)	B3LYP /SDD		B3LYP/6-311G(d,p)	B3LYP /SDD
C1	0.104	-0.096	O3	O3	-0.480
C2	0.051	-0.102	O7	O7	-0.525
C4	-0.175	-0.536	O10	O10	-0.443
C5	-0.156	0.194	013	013	-0.337
C8	-0.120	0.203	O17	O17	-0.469
C9	0.157	0.130	O19	O19	-0.513
C11	-0.090	-0.587	027	027	-.0.404
C12	0.249	-0.233	N26	N26	0.23
C14	-0.187	0.451	H28	H28	0.220
C15	-0.087	-0.554	H33	H33	0.389
C16	0.169	0.194	H35	H35	0.275
C18	0.124	0.135	H38	H38	0.379
C20	-0.096	-0.308	H40	H40	0.265
C22	0.015	-0.117	H42	H42	0.172
C24	-0.269	-0.493	H44	H44	0.239
C25	0.347	-0.155	H46	H46	0.387

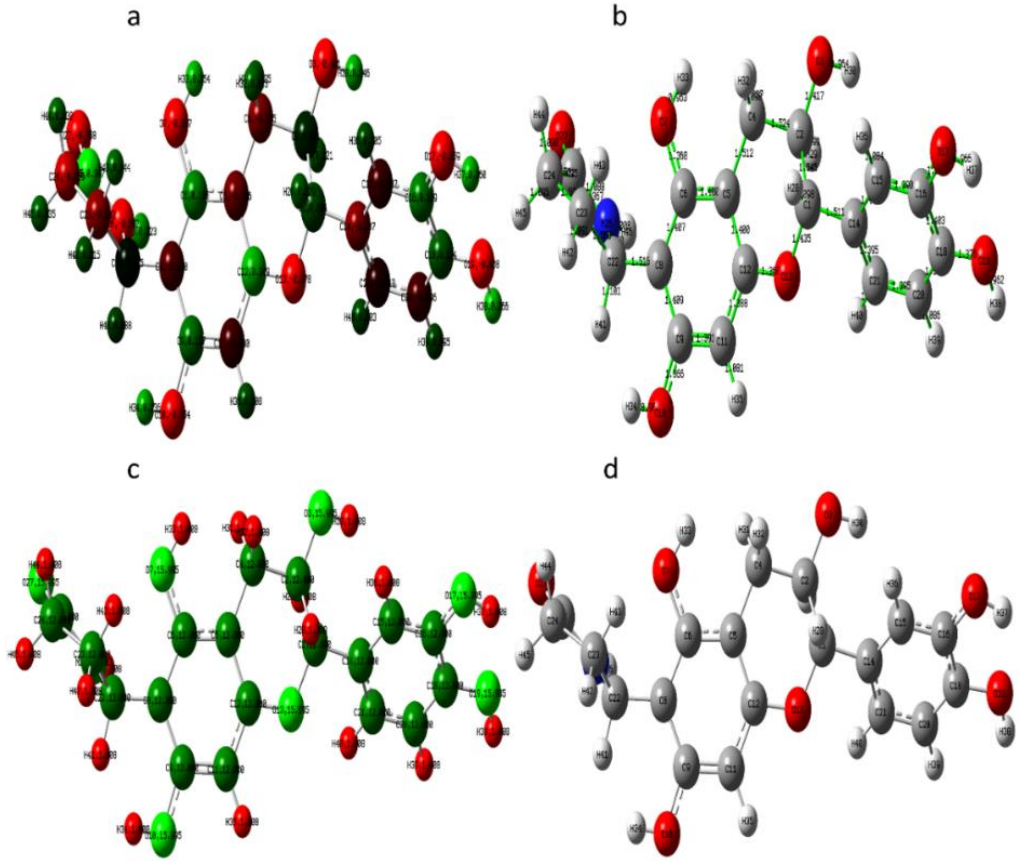

Figure 4. PEP molecule with DFT/B3LYP/6-311G(d,p) basis set a) mulliken b) bond length c) atomic mass d) structure optimization

3.6. NBO Analizi

Charge transfer interactions inside bonds are investigated using natural bond trajectory (NBO) analysis. NBO has been measured using the B3LYP/6-311G (d,p) basis set to the PEP compound [29]. The interaction energy is used to calculate the off-diagonal NBO Fock matrix components F(ij) [30]. This may be calculated using the quadratic perturbations method [31]. From the NBO analysis, monocentric lone pairs and dicentric bonds give a chemical bond's precise representation to a stable molecular species corresponding to a single Lewis formula [32]. The un-Lewis structure, the un-empty valence bond (LP) and the extravalence shelled Rydberg (RY*) orbitals can be seen valence anti-bonds (BD). The absence of Lewis-type NBOs (lone pairs and bonds) expressing the density matrix may be identified by the occupancy of these NBOs.

$$E(2) = \Delta Eij = qi \frac{(Ei,j)}{(Ej - Ei)}^{2}$$

Hyper-conjugative interactions' The energy is denoted by E (2). On an NBO basis, qi denotes the occupancy of the donating orbital, I and j. denote the energies of the accepting and giving orbitals, and Fij denotes the Fock matrix's off-diagonal element. The occupancy of the contributing (Lewis type) orbital is represented by qi, the energies of the giving and accepting orbitals are represented by i and j., and the off-diagonal element of the Fock matrix is represented by Fij. The B3LYP/6-311 basis set was used to calculate molecule PEP, electron density delocalization and intermolecular hybridization in NBO. As shown in Table 5, (C5-C6) diffuse's the intermolecular hype-conjugative interaction to σ* (C6-C8), resulting in a 5.62 KJ/mol stabilization. The molecule's the highest and most important energy

is π*(C5-C6) electron donation to the anti-bond acceptor acceptor, which has 26.89 KJ/mol's a stabilization energy from π(C8-C9).

Table 5. NBO findings selected for PEP utilizing the B3LYP / 6-311 G (d, p) theory level to illustrate the production of Lewis and non-Lewis orbitals.

NBO(i)	Type	ED/e	NBO(j)	Type	ED//e	E(2)[a] (Kcal/mol)	E (j)-E(i)[b] (a.u.)	F (i, j)[c] (a.u)
C1-C2	Σ	1.96932	C14-C21	σ*	0.02521	2.27	0.65	0.042
C1-O13	Σ	1.98423	C11-C12	σ*	0.02088	2.46	1.40	0.052
C1-C14	Σ	1.96729	C15-C16	σ*	0.02223	2.49	1.20	0.049
C11-H28	Σ	1.97401	C14-C21	σ*	0.02521	3.49	1.09	0.055
C2-C4	σ	1.97145	C5-C6	σ*	0.03207	3.32	1.19	0.056
C4C5	Σ	1.96919	C6-C8	σ*	0.03088	3.25	1.18	0.055
C5-C6	Σ	1.96811	C5-C12	σ*	0.03580	4.58	1.27	0.068
C5-C6	Σ	1.96811	C6-C8	σ*	0.03088	5.62	1.26	0.075
C5-C6	Σ	1.96811	C12-O13	σ*	0.02917	4.31	1.07	0.061
C5-C6	Π	1.68162	C8-C9	π *	0.44278	13.18	0.29	0.057
C5-C6	π	1.68162	C11-C12	π*	0.40600	26.63	0.29	0.080
C5-C12	σ	1.96999	C5-C6	σ*	0.03207	4.40	1.26	0.067
C5-C12	σ	1.96999	C11-C12	σ*	0.02088	5.16	1.28	0.073
C6-C8	σ	1.96410	C9-O10	σ*	0.02158	4.17	1.04	0.059
O7-H33	σ	1.98777	C6-C8	σ*	0.03088	4.15	1.30	0.066
C8-C9	σ	1.96949	C9-C11	σ*	0.02102	4.69	1.27	0.069
C8-C9	π	1.68000	C5-C6	π*	0.42699	26.89	0.28	0.080
C8-C9	π	1.68000	C9-C9	π*	0.44278	13.58	0.29	0.057
C8-C9	π	1.68000	C22-N26	σ*	0.03481	4.95	0.61	0.053
C11-C12	π	1.68465	C5-C6	π*	0.03207	14.71	0.28	0.059
C11-C12	π	1.68465	C8-C9	π*	0. 44278	26.85	0.28	0.080
C14-C21	π	1.68523	C15-C16	π*	0.38576	19.19	0.28	0.066
C14-C21	π	1.68523	C18-C20	π*	0.39535	20.06	0.27	0.067
C15-C16	π	1.67176	C14-C21	π*	0.37352	21.01	0.30	0.072
C15-C16	π	1.67176	C18-C20	π*	0. 39535	19.62	0.28	0.068
C18-C20	π	1.70086	C14-C21	π*	0. 37352	18.33	0.31	0.068
C18-C20	π	1.70086	C15-C16	π*	0.38576	19.11	0.30	0.069

[a]E (2) means the energy of hyper conjugative interaction (stabilization energy).
[b] Energy difference between donor and acceptor i and j NBO orbitals.
[c] F(i, j) is the Fock matrix element between i and j NBO orbitals

3.7. Molecular Docking Studies

Molecular docking's the *in silico* approach is used to recognize the interaction between ligands and proteins [33-35]. As a consequence of the PEP-AChE insertion work, Figure 5 shows their interaction in 2D and 3D modes. As a consequence of, the slip score was determined to be -7.105 cal/mol with PEP-AChE in Table 6. The bonding mechanism is ASP-74 (1.65 Å) and TYR-341 (2.58 Å) Hydroxyl-bonded Conventional Hydrogen Bond, TYR-341 (2.51 Å) Hydrogen Bond, PHE-295 (1.79 Å) and VAL-294 (2.51Å) Oxygen-bound and trational Hydrogen Bond in hydroxyl, Carbon-bound and hydrogen bond, LEU-76 (5.25 Å) Examples of Pi-alkyl bonds attached to Phenyl ring's the 2nd center and other interactions are as in Figure 5. Figure 5 shows a three-dimensional picture of the hydrogen bond donor/acceptor surface of the receptor.

Table 6. Docking score of PEP - AChE and PEP - BChE

Compound	Docking Score	
	AChE (PDB:4M0E)	BChE (PDB:6SAM)
PEP	-7.105	-7.784

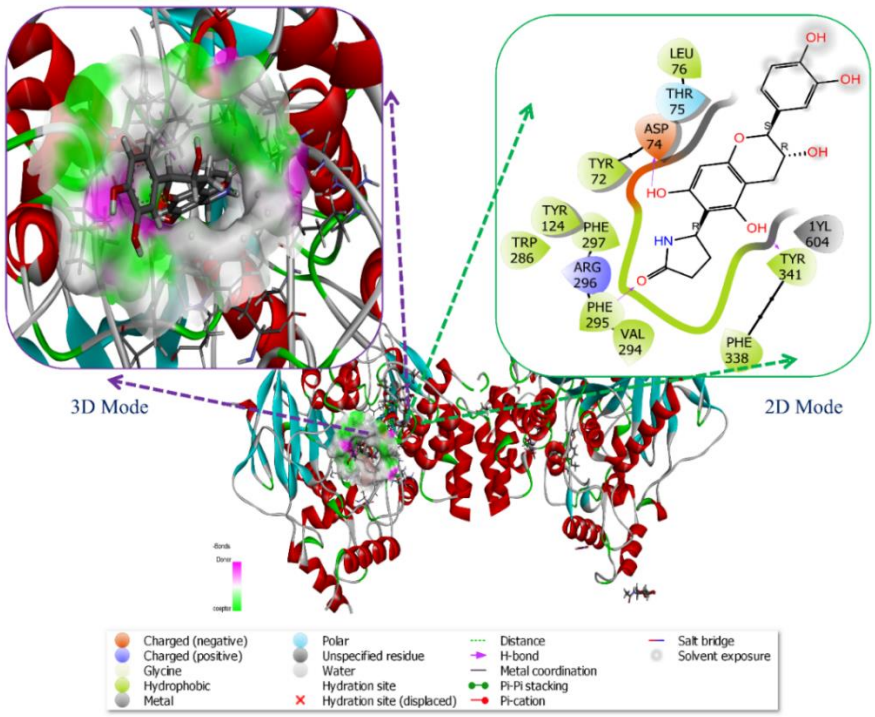

Figure 5. PEP-AChE interactions in 2D, and the receptor's aromatic surface in 3D.

As a consequence of BChE settlement work is like the 3D and 2D view in figure 6. As a result of binding with PEP-BDhE, the slip score was determined as -7.784 cal/mol in Table 6. ASP-70 (4.13 Å), PRO-285 (4.73), GLY-78 (4.47) and HIS-438 (3.73 Å) Conventional Hydrogen Bonding in Hydroxyl, PHE-329 (6.10 Å) and TRP-82 (6.03) 1. Pi-Pi T-shaped bonded to the phenyl ring, ALA-328 (5.56) and TYR-332 (5.75) attached to the center of the benzene ring are Pi-alkyl bond's examples. Other interactions are as in Figure 6.

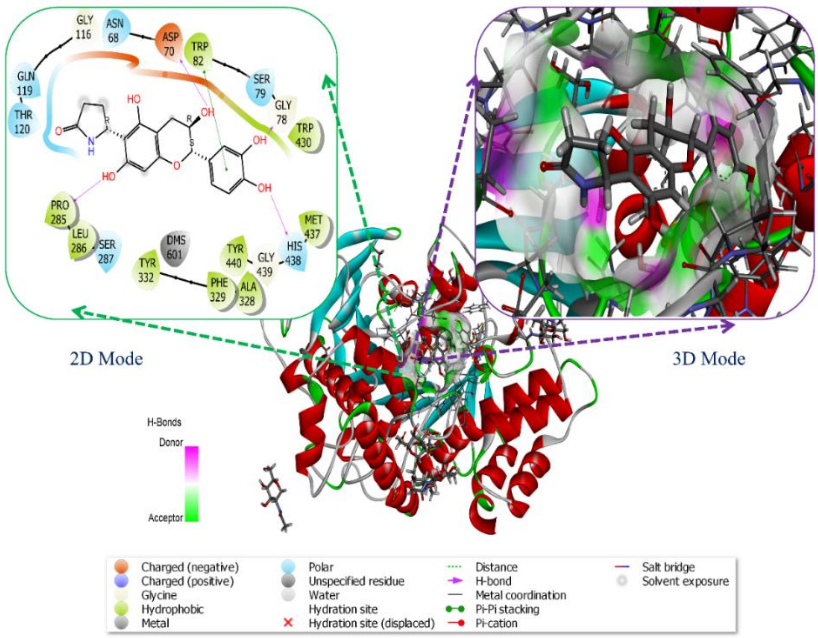

Figure 6. 2D picture of PEP - BChE interactions and 3D view of the receptor's aromatic surface.

4. CONCLUSION

In this study, a detailed theoretical analysis of PEP molecule was performed. DFT was used to analyze the structural characteristics utilizing the B3LYP exchange correlation functional, the SDD and 6-311G(d,p) basis sets.The parameters optimized, especially dihedral angles, bond angles and bond length have been calculated and shown to have a high correlation with the reference values. To determine the chemical stability, the compound's the reactivity, boundary molecular orbitals and molecular which based different electron intensive like total energy (E), polarizability (α), dipole moment (d), electronegativity (χ), chemical hardness and (η) electrophilicity (ω) used features. The LUMO and the HOMO's the energy have been calculated using DFT calculations with a base set. NBO analysis was utilized to determine quality and the charge distribution of optimized chemical structures. The highest stabilization energy value for the PEP compound was found as 26.89, 26.63 and 26.62 Kcal/mol, respectively. According to the NLO study, the molecule exhibited strong optical properties in various directions. The isotropic polarizability of the compound was found as 2.151 $x10^{-9}$ esu in the B3LYP/6-311G(d,p) method and 1.093$x10^{-9}$ esu in the B3LYP/SDD method. The molecule has a high ability to associate with AChE and BChE proteins according to molecular docking simulation. In the study, it was shown that the binding affinity shift scores with PEP–AChE and PEP–BChE were more effective with -7.105 cal/mol and -7.784 cal/mol and PEP–AchE receptor binding score, respectively. It could be investigated that the molecule may be a suitable candidate for innovation in medical applications, anti-cancer drugs with high potency and low side effects, and drugs used in Alzheimer disease's treatment.

CONFLICT OF INTEREST

There are no conflicts of interest as to publication of this article.

REFERENCES

[1] Ilkei V, Spaits A, Prechl A, Müller J, Könczöl Á, Lévai S, Riethmüller E, Szigetvári Á, Béni Z, Dékány M, Martins A, Hunyadi A, Antus S, Szántay C, Balogh GT, Kalaus G, Bölcskei H, and Hazai L, C8-selective biomimetic transformation of 5,7-dihydroxylated flavonoids by an acid-catalysed phenolic Mannich reaction: Synthesis of flavonoid alkaloids with quercetin and (–)-epicatechin skeletons. Tetrahedron.2017; 73:(11): p. 1503-1510.

[2] Moyeenudin HM, Thiruchelvi R, Wilfred Lawrence A, and John Williams R, The phytochemical components of caesalpinia sappan in treating respiratory ailments through an herbal soup in addition with sensory evaluation. Materials Today: Proceedings.2022; 56: p. 2167-2171.

[3] Xiao P-t, Liu S-y, Kuang Y-j, Jiang Z-m, Lin Y, Xie Z-s, and Liu EH, Network pharmacology analysis and experimental validation to explore the mechanism of sea buckthorn flavonoids on hyperlipidemia. Journal of Ethnopharmacology.2021; 264: p. 113380.

[4] Miao N, Yun C, Han S, Shi Y, Gao Y, Wu S, Zhao Z, Wang H, and Wang W, Postharvest UV-A radiation affects flavonoid content, composition, and bioactivity of Scutellaria baicalensis root. Postharvest Biology and Technology.2022; 189: p. 111933.

[5] Mora-Granados M, Crevillen AG, González-Gómez D, and Gallego-Picó A, Disposable electrochemical sensor combined with molecularly imprinted solid-phase extraction for catabolites detection of flavan-3-ol in urine samples. Talanta.2021; 235: p. 122734.

[6] Wojdyło A and Nowicka P, Anticholinergic effects of Actinidia arguta fruits and their polyphenol content determined by liquid chromatography-photodiode array detector-

quadrupole/time of flight-mass spectrometry (LC-MS-PDA-Q/TOF). Food Chemistry.2019; 271: p. 216-223.

[7] Webby RF, Wilson RD, and Ferguson AR, Leaf flavonoids of Actinidia. Biochemical Systematics and Ecology.1994; 22:(3): p. 277-286.

[8] Teng J, Li J, Zhao Y, and Wang M, Hesperetin, a dietary flavonoid, inhibits AGEs-induced oxidative stress and inflammation in RAW264.7 cells. Journal of Functional Foods.2021; 81: p. 104480.

[9] Frisch MJ, Trucks GW, and SH, and GE. S, Gaussian 09. Revision E.01.

[10] Tunç G, Canımkurbey B, Dedeoğlu B, Zorlu Y, Eryılmaz S, and Gürek AG, Synthesis, crystal structure and electronic applications of monocarboxylic acid substituted phthalonitrile derivatives combined with DFT studies. Journal of Molecular Structure.2021; 1240: p. 130545.

[11] Anuoluwa Bamidele E, Olanrewaju Ijaola A, Bodunrin M, Ajiteru O, Martha Oyibo A, Makhatha E, and Asmatulu E, Discovery and prediction capabilities in metal-based nanomaterials: An overview of the application of machine learning techniques and some recent advances. Advanced Engineering Informatics.2022; 52: p. 101593.

[12] Solğun DG, Yıldıko Ü, and Ağırtaş MS, Synthesis, DFT Calculations, Photophysical, Photochemical Properties of Peripherally Metallophthalocyanines Bearing (2-(Benzo[d] [1,3] Dioxol-5-Ylmethoxy) Phenoxy) Substituents. Polycyclic Aromatic Compounds.2021: p. 1-19.

[13] Sonia C, Devi TG, and Karlo T, DFT study on the structural and chemical properties of Janus kinase inhibitor drug Baricitinib. Materials Today: Proceedings.2022.

[14] Fatima A, Khanum G, Verma I, Butcher RJ, Siddiqui N, Srivastava SK, and Javed S, Synthesis, Characterization, Crystal Structure, Hirshfeld Surface, Electronic Excitation, Molecular Docking, and DFT Studies on 2-Amino Thiophene Derivative. Polycyclic Aromatic Compounds.2022.

[15] Kole PB, Kollur SP, Revanasiddappa HD, Shivamallu C, Costa RA, Junior ESA, Anselmo LM, da Silva JN, Srinivasa C, Syed A, and Singh FV, Structural, Electronic, Vibrational and Pharmacological Investigations of Highly Functionalized Diarylmethane Molecules Using DFT Calculations, Molecular Dynamics and Molecular Docking. Polycyclic Aromatic Compounds.2022.

[16] Soni K, Saxena S, and Jain A, Recent advances in DFT assisted optimized energy, stability and distortions of optimized topologies of certain biopotent dimethyltin(IV) complexes. Journal of the Indian Chemical Society.2022; 99:(3): p. 100332.

[17] Budania S, Saxena S, and Jain A, Assessment of DFT based optimized molecular structure-antioxidant efficacy relationship of trimethylgermanium(IV) complexes. Journal of the Indian Chemical Society.2022; 99:(5): p. 100419.

[18] Solğun DG, Keskin MS, yıldıko Ü, and Ağırtaş MS, DFT analysis and electronic properties, and synthesis of tetra (9-phenyl-9H-xanthen-9-yl) oxy peripheral-substituted zinc phthalocyanine. Chemical Papers.2020; 74:(8): p. 2389-2401.

[19] Janeoo S, Reenu, Saroa A, Kumar R, and Kaur H, Computational investigation of bioactive 2,3-diaryl quinolines using DFT method: FT- IR, NMR spectra, NBO, NLO, HOMO-LUMO transitions, and quantum-chemical properties. Journal of Molecular Structure.2022; 1253: p. 132285.

[20] Buvaneswari M, Santhakumari R, Usha C, Jayasree R, and Sagadevan S, Synthesis, growth, structural, spectroscopic, optical, thermal, DFT, HOMO–LUMO, MEP, NBO analysis and thermodynamic properties of vanillin isonicotinic hydrazide single crystal. Journal of Molecular Structure.2021; 1243: p. 130856.

[21] Janani S, Rajagopal H, Muthu S, Aayisha S, and Raja M, Molecular structure, spectroscopic (FT-IR, FT-Raman, NMR), HOMO-LUMO, chemical reactivity, AIM, ELF, LOL and Molecular docking studies on 1-Benzyl-4-(N-Boc-amino)piperidine. Journal of Molecular Structure.2021; 1230: p. 129657.

[22] Akman ME, Ata AÇ, Yıldıko Ü, and, Cakmak İ, and Molecular structure, frontier molecular orbitals, NBO, MESP and thermodynamic properties of 5, 12-dibromo perylene with DFT calculation methods. International Journal of Chemistry Technology.2020; 4:(1): p. 49-59.

[23] Sevvanthi S, Muthu S, Aayisha S, Ramesh P, and Raja M, Spectroscopic (FT-IR, FT-Raman and UV-Vis), computational (ELF, LOL, NBO, HOMO-LUMO, Fukui, MEP) studies and molecular docking on benzodiazepine derivatives- heterocyclic organic arenes. Chemical Data Collections.2020; 30: p. 100574.

[24] Kargar H, Fallah-Mehrjardi M, Behjatmanesh-Ardakani R, and Munawar KS, Synthesis, spectra (FT-IR, NMR) investigations, DFT, FMO, MEP, NBO analysis and catalytic activity of MoO2(VI) complex with ONO tridentate hydrazone Schiff base ligand. Journal of Molecular Structure.2021; 1245: p. 131259.

[25] Raveendiran C, Prabukanthan P, Ragavendran V, Harichandran G, Dinakaran K, and Seenuvasakumaran P, Synthesis, crystal growth, crystal investigation, optical, thermal, DFT and NLO studies of 2-methylanilinium- 4-methylbenzenesulfonate organic single crystal: Experimental and computational approach. Materials Today: Proceedings.2022.

[26] Remiya JP, Sikha TS, Shyni B, Anitha L, Lakshmi CSN, and Jayasree EG, Synthesis, spectral characterization and biological evaluations with DFT analysis on molecular geometry and NLO of 1,4,7,10-tetraazacyclotetradecane-11,14-dione. Journal of the Indian Chemical Society.2021; 98:(9): p. 100132.

[27] Priya MK, Revathi BK, Renuka V, Sathya S, and Asirvatham PS, Molecular Structure, Spectroscopic (FT-IR, FT-Raman, 13C and 1H NMR) Analysis, HOMO-LUMO Energies, Mulliken, MEP and Thermal Properties of New Chalcone Derivative by DFT Calculation. Materials Today: Proceedings.2019; 8: p. 37-46.

[28] Arivazhagan M and Senthil kumar J, Molecular structure, vibrational spectral assignments, HOMO–LUMO, MESP, Mulliken analysis and thermodynamic properties of 2,6-xylenol and 2,5-dimethyl cyclohexanol based on DFT calculation. Spectrochimica Acta Part A: Molecular and Biomolecular Spectroscopy.2015; 137: p. 490-502.

[29] Sakr MAS and Saad MA, Spectroscopic investigation, DFT, NBO and TD-DFT calculation for porphyrin (PP) and porphyrin-based materials (PPBMs). Journal of Molecular Structure.2022; 1258: p. 132699.

[30] Murugan P, Jeyavijayan S, Ramuthai M, and Narmadha RB, Structural, Spectroscopic, NBO and Molecular Docking Analysis of 5-Nitrobenzimidazole – A DFT Approach. Polycyclic Aromatic Compounds.2022.

[31] Jebasingh Kores J, Antony Danish I, Sasitha T, Gershom Stuart J, Jimla Pushpam E, and Winfred Jebaraj J, Spectral, NBO, NLO, NCI, aromaticity and charge transfer analyses of anthracene-9,10-dicarboxaldehyde by DFT. Heliyon.2021; 7:(11): p. e08377.

[32] Trabelsi S, Tlili M, Abdelmoulahi H, Bouazizi S, Nasr S, González MA, Bellissent-Funel M-C, and Darpentigny J, Intermolecular interactions in an equimolar methanol-water mixture: Neutron scattering, DFT, NBO, AIM, and MD investigations. Journal of Molecular Liquids.2022; 349: p. 118131.

[33] Kaya ED, Türkhan A, Gür F, and Gür B, A novel method for explaining the product inhibition mechanisms via molecular docking: inhibition studies for tyrosinase from Agaricus bisporus. Journal of Biomolecular Structure and Dynamics.2021: p. 1-14.

[34] Altun K, Yıldıko Ü, Tanrıverdi AA, Çakmak İJIJoC, and Technology, Structural and spectral properties of 4-(4-(1-(4-Hydroxyphenyl)-1-phenylethyl) phenoxy) phthalonitrile: Analysis by TD-DFT method, ADME analysis and docking studies. 5:(2): p. 147-155.

[35] Madadi Mahani N, Mostaghni F, and Shafiekhani H, Cuspareine as alkaloid against COVID-19 designed with ionic liquids: DFT and docking molecular approaches. Journal of Photochemistry and Photobiology B: Biology.2022; 231: p. 112447.